Hindawi
Journal of Nanomaterials
Volume 2021, Article ID 3199949, 6 pages
https://doi.org/10.1155/2021/3199949

*Research Article*

# Synthesis and Characterization of the Chitosan Silver Nanoparticle-Reinforced *Borassus flabellifer* Trichome- and *Prosopis juliflora* Wood-Based Nanocomposite for Environmental Application

**Ch. Nanda Krishna**,[1] **Madhavi Katamaneni**,[1] **Kalyan Chakravarti Yelavarti**,[1] **B. Sobhan Babu**,[2] **B. Ravi Kumar**,[3] **and M. Viju Prakash**[4]

[1]*Department of Information Technology, VR Siddhartha Engineering College, Kanuru, Vijayawada, Andhra Pradesh 520007, India*
[2]*Department of Information Technology, Gudlavalleru Engineering College, Gudlavaleru, Andhra Pradesh 521356, India*
[3]*Department of ECE, Institute of Aeronautical Engineering, Dundigal, 500043 Telangana, India*
[4]*Department of Computer Science, Kombolcha Institute of Technology, Wollo University, P.O. Box 208, Ethiopia*

Correspondence should be addressed to Ch. Nanda Krishna; nkcherukuri@gmail.com
and M. Viju Prakash; vijuprakash@kiot.edu.et

Received 18 August 2021; Revised 24 September 2021; Accepted 4 October 2021; Published 22 October 2021

Academic Editor: Lakshmipathy R



Wood is a wide flexible material appreciated extremely for its cost-effectiveness, great quantity, and biocompatibility. In addition, naturally existing materials possess prominent biomedical applications, and they can withstand efficiently when compared to other materials like glass, steel, and plastics. The present study revealed the prepared chitosan, silver nanoparticles incorporated with *Borassus flabellifer* trichome, and fabrication of *Prosopis juliflora* wood-based biomaterial. A characterization study was done by UV-visible spectroscopic analysis, FTIR analysis, and SEM analysis expressing and confirming a significant characteristic and morphological property of the prepared biomaterial.

## 1. Introduction

Wood is a wide natural reusable material which is important in different industries making the researchers to work on it [1]. The naturally existing porous wood acts as a good carrier to build a functional composite that is still rarely used. Nanotechnology is a promising area to enhance the efficiency and effectiveness towards different bioremediation processes. Its improved reactivity and increased surface area to volume ratio had great impact when compared with those bulk materials [2]. The physical characteristic of chitosan is its flexibility, and studies regarding its properties have been performed and the outcome is very positive [3]. This latest material has its durability, biodegradability, biocompatibility, nontoxicity, and adsorption in pharmaceuticals, agriculture, forestry, skincare products, and food and water treatment applications. Still, it is emerging as an innovator in textiles, health care and pharmaceuticals [4].

In India, the palmyra tree is the official tree of Tamil Nadu. In tradition, it is called askarpaha, a celestial tree, nudged and extremely cherished by the people, and considered a god [5]. Borassus flabellifer includes innumerable essential constituents, gums, fats, albuminoids, carbohydrates were investigated [6]. Silver nanoparticles are considered to have a strong and wide range of therapeutic applications, and even low concentration of silver nanoparticles has been found, in some cases, to possess strong potential to treat a variety of diseases [7]. A nanocomposite is one of the unusual composite materials that are shown to possess a capability of being used as a biometric sensor as well as in numerous treatment protocols. Silver nanoparticle (AgNP) incorporation has a great impact on the water purification

process due to its stability, chemical catalytic ability, low toxicity to humans, and effective antimicrobial property [8].

The present investigation strongly focused on the preparation and characterization of the *Borassus flabellifer* trichome and *Prosopis juliflora* wood, silver nanoparticles (AgNPs), and chitosan with different proportions by UV-visible spectroscopic analysis, FTIR analysis, and SEM analysis.

## 2. Materials and Methodology

*2.1. Chemicals and Samples.* From Sigma-Aldrich Chemical Company, USA, the required fine chemicals like silver nitrate were purchased and all other requirements are of first-class analytical grade.

*2.2. Preparation of Chitosan Solution (Ch).* The purified chitosan was significantly obtained by performing alkaline deacetylation of chitin from crab shells. The mixture was obtained by dissolving 1 gram of chitosan in 100 ml of 0.25 N hydrochloric acid.

*2.3. Preparation of the Borassus flabellifer Trichome-Chitosan Biocomposite (TC-Ch).* In 50 ml double distilled water, 1 g of *Borassus flabellifer* trichome and 1% chitosan (Ch) were mixed to this solution [9]. The pH of the solutions was adjusted to 7.0, and the resultant materials were used for further use. It was denoted as TC-Ch [10].

*2.4. Preparation of Silver Nanoparticle (AgNP) Solution.* Silver nanoparticles were prepared by using a modified method of Turkevich. In brief, 30 ml of 1 mM silver nitrate solution was boiled and kept in a magnetic stirrer. Once it starts to boil, add 3 ml of 10 mM trisodium citrate in the ratio of one drop per second and wait till it change into brown color. Finally, it is denoted as AgNPs [11].

*2.5. Preparation of the Wood Sample (W).* The wood pieces were collected from *Prosopis juliflora*, and the hardwood of the plant was finely powdered. The obtained finely powdered wood sample was collected, and it is denoted as W [12].

*2.6. Incorporation of AgNPs and W into the TC-Ch Biocomposites (TC-Ch-AgNPs-W).* The prepared TC-Ch biocomposite was soaked in solution having 0.01% of AgNPs and wood sample for about 24 hrs. Silver nanoparticle- (AgNP-) and wood-integrated TC-Ch was taken and dried at 37°C [13]. The obtained material was expressed as TC-Ch-Ag-W.

*2.7. Characterization Studies.* The characterization studies were performed for *Prosopis juliflora* wood (W), *Borassus flabellifer* trichome- (TC-) prepared AgNPs, Ch, TC-AgNPs, TC-W, TC-Ch, TC-Ch-AgNPs, and TC-Ch-AgNPs-W [14].

*2.8. UV-Visible Spectrometric Analysis.* A UV-visible spectrum was obtained for different samples observed using a UV-visible spectrophotometry analysis for authentication of availability of the desired/formed molecule. The deionized water was used as a blank.

*2.9. FTIR Analysis.* IR provides significant data on the rotational and vibrational motion of the specific molecules, and it improves the effective identification and characterizations of the obtained composite interactions evaluated under FTIR to observe structural conformation [15]. All the required measurements were carried out in the range of 400 to 4000 $cm^{-1}$.

*2.10. Morphology Observation.* The morphological experiment was performed for TC-Ch-AgNPs and TC-Ch-AgNPs-W by using a JEOL JSM-7401F scanning electron microscope.

## 3. Result and Discussion

From the present investigation, *Prosopis juliflora* wood (W), *Borassus flabellifer* trichome (TC), silver nanoparticles (AgNPs), and chitosan (Ch) with incorporation of TC-AgNP, TC-W, TC-Ch, TC-Ch-AgNP, and TC-Ch-AgNP-W composites have been prepared by a modified method of the available literature and were systematically partially characterized by UV spectroscopy, FTIR spectroscopy, and SEM analysis, and the obtained results were interpreted with the available literature.

*3.1. UV-Visible Spectroscopic Analysis.* The optical properties of TC, AgNPs, Ch, W, TC-AgNPs, TC-W, TC-Ch, TC-Ch-AgNPs, and TC-Ch-AGNPs-W were experimented by using UV-visible spectroscopy, and the obtained results are shown in Figures 1–3. The obtained spectrum broad absorption band intensity was compared with that of different proportions like TC, AgNPs, Ch, W, TC-AgNPs, TC-W, TC-Ch, TC-Ch-AgNPs, and TC-Ch-AGNPs-W [16].

The UV-visible spectroscopy analysis for TC, W, Ch, and AgNPs is represented in Figure 1 with the absorptive peak at 282 nm, 285 nm, 320 nm, and 400 nm in the UV region.

The UV-visible spectroscopy analysis was performed for TC-W, TC-Ch, and TC-AgNPs and is represented in Figure 2. Here, *Borassus flabellifer* trichomes (TC) act as a base for Ch, W, and AgNPs. From the obtained results, the absorptive peak was observed at 280 nmin all three different compositions [17].

The biocomposites TC-Ch-AgNPs and TC-Ch-AGNPs-W were subjected to UV-visible spectroscopy analysis to determine the optical property which is represented in Figure 3. It indicated that TC-Ch-AgNPs is not showing any absorptive peak and TC-Ch-AGNPs-W exhibits a peak at 300 nm [18].

From Figure 3, it represents that when four different components (TC, Ch, AgNPs, and W) were mixed, the interaction between one and other molecules with the 1 : 1 ratio has been successfully achieved to form a single bionanomaterial [19]. From the above results, the absorptive peak confirmed that TC acts as a base for the incorporation of Ch, AgNPs, and W.

*3.2. FTIR Spectroscopic Analysis.* The significant vibrational patterns acquired from FTIR spectroscopic analysis offer the existing functional groups such as nitrogen, carbon,

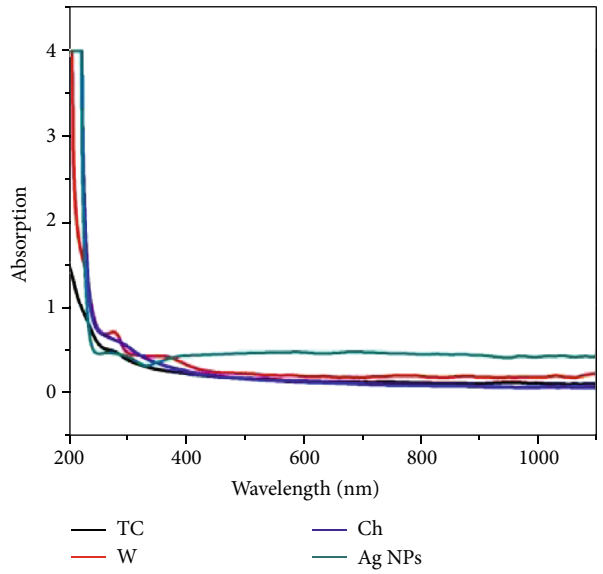


Figure 1: UV-visible spectroscopy analysis for TC, W, Ch, and AgNPs.

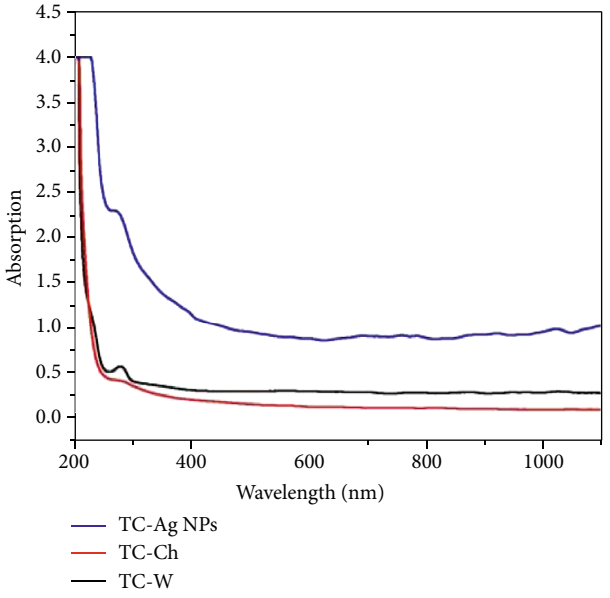


Figure 2: UV-visible spectroscopy analysis for TC-W, TC-Ch, and TC-AgNPs.

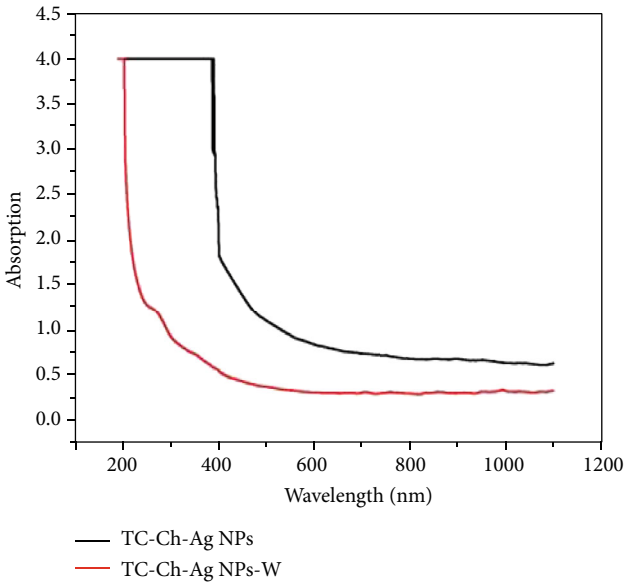


Figure 3: UV-visible spectroscopy analysis for TC-Ch-AgNPs and TC-Ch-AGNPs-W.

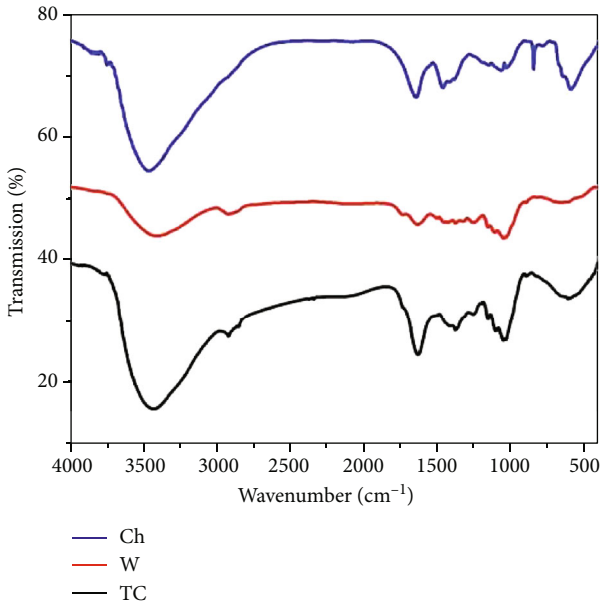


Figure 4: FTIR spectroscopy analysis for TC, W, Ch, and AgNPs.

and oxygen in different samples (TC, Ch, W, TC-AgNPs, TC-W, TC-Ch, TC-Ch-AgNPs, and TC-Ch-AGNPs-W). The FTIR spectroscopic analysis was performed, and the characteristic peak was obtained in the range between 4000 and 500 cm$^{-1}$. The obtained results are presented in Figures 4–6, and they were interpreted with the available literature [20].

For the chief functional groups for chitosan, a characteristic peak was obtained at 3500 to 3300 cm$^{-1}$ and was attributed to the O-H group of vibrational spreads. Figure 4 shows the FTIR spectroscopy analysis for TC, W, Ch, and AgNPs. The C-H bending vibration of the alkyl group and the N-H bending vibration of the protonated amino ($-NH_2$) group are attributed to absorption peaks at 1630 cm and 1531 cm$^{-1}$. The peaks at 1059 and 886 cm$^{-1}$ by the glucopyranose ring of the chitosan matrix and antisymmetric detention vibration of C-O-C-bridges are allocated.

The FTIR analysis (Figure 5) for W has shown O-H vibrations with approximately 3200-3600 cm$^{-1}$. Carboxylic acids of the O-H stretch occur at 290836 cm$^{-1}$ of the *P. juliflora* and 173845 cm$^{-1}$ of the C=O stretch. The 1373 cm$^{-1}$ peak is designed for W with an aromatic amino group of strong C-N stretches. Populations were collected in the C-N alcohol stretch at 1158 cm$^{-1}$, 1111 cm$^{-1}$, and 1053 cm$^{-1}$

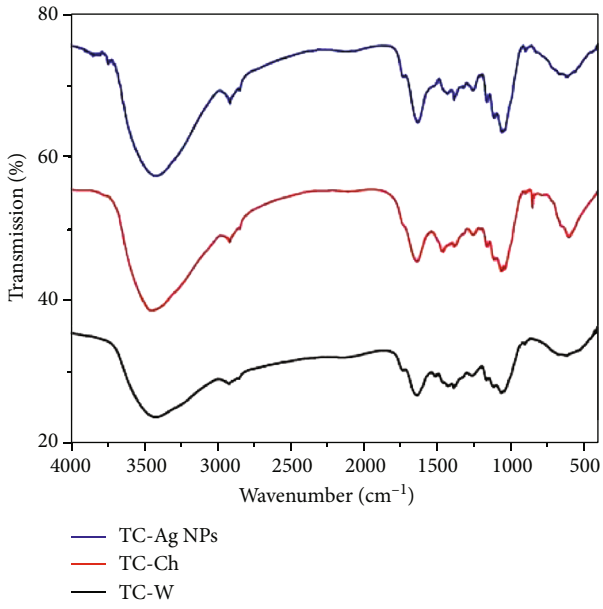


Figure 5: FTIR spectroscopy analysis for TC-W, TC-Ch, and TC-AgNPs.

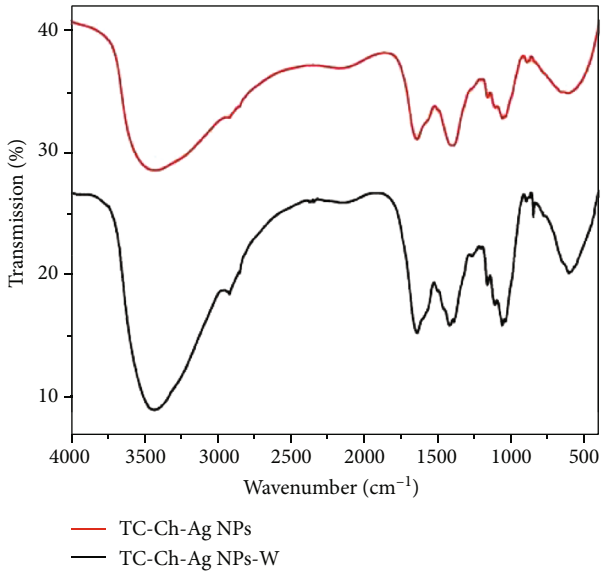


Figure 6: FTIR spectroscopy analysis for TC-Ch-AgNPs and TC-Ch-AGNPs-W.

[21]. The 1400-600 cm$^{-1}$ area has a peculiar pattern of absorption in this region, which is often called a region of fingerprinting because the fingerprints of an individual are unique. Carboxylic acids, amines, and compounds are responsible for hydroxy replacements.

The characteristic FTIR analysis exhibits the TC peak as the parameter went up in 3500 cm$^{-1}$, the chitosan molecule shifted to 3000 cm$^{-1}$, and a simple O-H stretching vibration was observed, attributable to the NH stretching of the main functional group. Figure 5 shows the FTIR spectroscopy analysis for TC-W, TC-Ch, and TC-AgNPs. The presence of absorption peaks at 1750 to 1.5 to 3.5H to 15.5 cm$^{-1}$ was triggered by the stretching of the N-protonated amino group

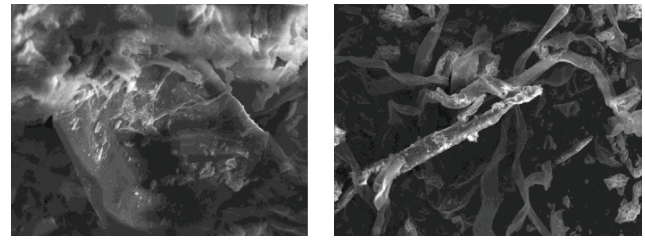


Figure 7: SEM images of (a) TC-Ch-AgNP and (b) TC-Ch-AgNP-W biocomposites.

and alkyl-group bending from 17.5 to 18.5 cm to 19.5 ppm. When the remaining amide groups have a bond stretching intensity of intermolecular bonds, the groups have an N-H vibration at a frequency of 1663.5 cm$^{-1}$, and when intermolecular bonds are involved, it is at 1500 cm$^{-1}$. The amide I peak at 1429.9 cm$^{-1}$, IH2N deformation, 1451.1 cm$^{-1}$, and 14.2 cm$^{-1}$ $NH_2$ is given a lifetime of 79 $\mu$s which is long [22]. The absorption peak occurs at 1405-680 cm$^{-1}$ due to the asymmetric vibration of the C-O-C bonds in the chitosan matrix and is interpreted as a glucosyl group due to the glucose rings.

For all three samples, TC-AgNPs, TC-W, and TC-Ch, the characteristic FTIR analysis shows the most similar peak with minor alteration. The three peaks at 3500 to 3000 cm$^{-1}$ were expressed having the main functional group of chitosan, which are due to the O-H group of stretching vibrations. The N-H bending vibration of the protonated amino group and C-H bending express the alkyl groups that are responsible for the peaks at 1750 to 1500 cm$^{-1}$. At 1663.5 cm$^{-1}$ and 1500 cm$^{-1}$ and 1659.5 cm$^{-1}$, respectively, the existing amide frequencies consist of the remaining acetamido groups' -C-O bond stretch and the N-H bending vibrations of the -$NH_2$ groups. -$NH_2$ deformation is responsible for the peaks at 1429.9 cm$^{-1}$, 1451.1 cm$^{-1}$, 1418.2 cm$^{-1}$, and 1419.1 cm$^{-1}$.

The characteristic FTIR analysis (Figure 6) shows that TC-Ch-AgNPs and TC-Ch-AGNPs-W show most similar peaks with slight modification. The changes were observed that TC-Ch-AgNPs peak was sharp compared then TC-Ch-AgNPs peak, and it was expressed that there was a formation of strong peak with a précised functional group at the peak which represented the above proportions.

*3.3. SEM Analysis.* SEM investigation gives strong impact to visualize the significant size and shape of the prepared biomaterial with the composition of TC-Ch-AgNPs and TC-Ch-AgNPs-W. The SEM images of these two composites are shown in Figures 7(a) and 7(b).

Figures 7(a) and 7(b) show the improved surface morphology of the prepared biomaterials TC-Ch-AgNPs and TC-Ch-AgNPs-W.

From Figures 7(a) and 7(b), one can clearly see the fibrous nature of chitin with the crumbles, as well as the silver particles and woody texture of the cuticle, particularly under a microscope. The trichome size ranges from 10 to 20 m particles that make up the vast majority of the surface

having a spherical shape, while some particles on the surface appear as single units, but the majority of the rest appears to be aggregated. At the lowest concentrations, silver particles are just about 45 nanometers in size, and the average size of the aggregated particles is about 64 nanometers. The wood sample size is around 55.54 nm, and the chitosan size is around 85.4 nm. SEM images clearly depict the presence of different molecules in the incorporated biomaterial.

## 4. Conclusion

The present investigation of UV and FTIR characteristic peaks was obtained for TC, Ch, W, TC-AgNPs, TC-W, TC-Ch, TC-Ch-AgNPs, and TC-Ch-AGNPs-W. The UV spectroscopic results expressed a significant peak confirming the presence of molecules. From the FTIR graph, the different functional groups were observed, and it was confirmed that the improved and strong peak was in TC-Ch-AGNPs-W. The SEM images for TC-Ch-AgNPs and TC-Ch-AGNPs-W improved the surface area scanning electron microscopic investigation. It shows the incorporation of Ch and AgNPs to W and TC. The morphograph exhibits fibrous nature with an improved surface area. From the prepared materials, it may have a great impact on the different applications. In addition, it also may offer different bioremediation processes with ecofriendly nature.

## Data Availability

The data used to support the findings of this study are included within the article. Should further data or information be required, these are available from the corresponding author upon request.

## Disclosure

The study was performed as a part of the employment in Kombolcha Institute of Technology, Wollo University, Kombolcha, Amhara, Ethiopia.

## Conflicts of Interest

The authors declare that there are no conflicts of interest regarding the publication of this paper.

## Acknowledgments

The authors thank the VR Siddhartha Engineering College, Vijayawada, and Institute of Aeronautical Engineering, Dundigal, for providing characterization support to complete this research work.

## References

[1] I. Hussain, N. B. Singh, A. Singh, H. Singh, and S. C. Singh, "Green synthesis of nanoparticles and its potential application," *Biotechnology Letters*, vol. 38, no. 4, pp. 545–560, 2016.

[2] S. Bhakya, S. Muthukrishnan, M. Sukumaran, and M. Muthukumar, "Biogenic synthesis of silver nanoparticles and their antioxidant and antibacterial activity," *Applied Nanoscience*, vol. 6, no. 5, pp. 755–766, 2016.

[3] M. Vidiella del Blanco, E. J. Fischer, and E. Cabane, "Underwater superoleophobic wood cross sections for efficient oil/water separation," *Advanced Materials Interfaces*, vol. 4, no. 21, pp. 170–184, 2017.

[4] J. J. Wang, Z. W. Zeng, R. Z. Xiao et al., "Recent advances of chitosan nanoparticles as drug carriers," *International Journal of Nanomedicine*, vol. 6, pp. 765–774, 2011.

[5] F. Chen, A. Gong, M. Zhu et al., "Mesoporous, three-dimensional wood membrane decorated with nanoparticles for highly efficient water treatment," *ACS Nano*, vol. 11, no. 4, pp. 4275–4282, 2017.

[6] J. Hai, F. Chen, J. Su, X. Fu, and B. Wang, "Porous wood members-based amplified colorimetric sensor for Hg2+ detection through Hg2+-triggered methylene blue reduction reactions," *Analytical chemistry*, vol. 90, no. 7, pp. 4909–4915, 2018.

[7] L. Cabrales, N. Abidi, and F. Manciu, "Characterization of developing cotton fibers by confocal Raman microscopy," *Fibers*, vol. 2, no. 4, pp. 285–294, 2014.

[8] F. Jiang, T. Li, Y. Li et al., "Wood-based nanotechnologies toward sustainability," *Advanced Materials*, vol. 30, no. 1, pp. 17034–17053, 2018.

[9] M. I. Niyas Ahamed, N. Gomathi, V. Ragul et al., "Novel preparation of chitosan from crab shell using probe sonicator and its antibacterial activity," *Journal of Academia and Industrial Research*, vol. 6, no. 8, pp. 133–136, 2018.

[10] C. A. Mecha and V. L. Pillay, "Development and evaluation of woven fabric microfiltration membranes impregnated with silver nanoparticles for potable water treatment," *Journal of membrane science*, vol. 458, pp. 149–156, 2014.

[11] N. Supraja, S. Thiruchenduran, and T. Prasad, "Synthesis and characterization of chitosan nanoparticles and evaluation of antimicrobial activity antioxidant activity," *Advancements in Bioequivalence & Bioavailability*, vol. 2, no. 1, pp. 88–94, 2018.

[12] S. Yogeshwaran, L. Natrayan, G. Udhayakumar, G. Godwin, and L. Yuvaraj, "Effect of waste tyre particles reinforcement on mechanical properties of jute and abaca fiber-epoxy hybrid composites with pre-treatment," *Materials Today: Proceedings*, vol. 37, no. 2, pp. 1377–1380, 2021.

[13] M. I. Niyas Ahamed, S. Sankar, P. Mohammed Kashif, S. K. Hayath Basha, and T. P. Sastry, "Evaluation of biomaterial containing regenerated cellulose and chitosan incorporated with silver nanoparticles," *International Journal of Biological Macromolecules*, vol. 72, pp. 680–686, 2015.

[14] H. M. Ericsson and J. C. Sherris, "Acta Pathologica," *Microbiologica Scandinavica*, vol. 217, 1971.

[15] L. H. Reddy, J. L. Arias, J. Nicolas, and P. Couvreur, "Magnetic nanoparticles: design and characterization, toxicity and biocompatibility, pharmaceutical and biomedical applications," *Chemical Reviews*, vol. 112, no. 11, pp. 5818–5878, 2012.

[16] P. Kumar, M. Govindaraju, S. Senthamilselvi, and K. Premkumar, "Photocatalytic degradation of methyl orange dye using silver (Ag) nanoparticles synthesized from *Ulva lactuca*," *Colloids and Surfaces, B: Biointerfaces*, vol. 103, pp. 658–661, 2013.

[17] M. Goudarzi, N. Mir, and M. Mousavi-Kamazani, "Biosynthesis and characterization of silver nanoparticles prepared from two novel natural precursors by facile thermal decomposition methods," *Scientific Reports*, vol. 6, no. 1, pp. 325–339, 2016.

[18] A. Soroush, W. Ma, Y. Silvino, and M. S. Rahaman, "Surface modification of thin film composite forward osmosis membrane by silver-decorated graphene-oxide nanosheets," *Nano*, vol. 2, no. 4, pp. 395–405, 2015.

[19] R. Suryanarayanan, V. G. Sridhar, L. Natrayan et al., "Improvement on mechanical properties of submerged friction stir joining of dissimilar tailor welded aluminum blanks," *Advances in Materials Science and Engineering*, vol. 2021, Article ID 3355692, 6 pages, 2021.

[20] R. Xing, H. Yu, S. Liu, Q. Zhang, Z. Li, and P. Li, "Preparation of low-molecular-weight and high-sulfate-content chitosans under microwave radiation and their potential antioxidant activity in vitro," *Carbohydrate research*, vol. 339, no. 15, pp. 2515–2519, 2004.

[21] S. Yogeshwaran, L. Natrayan, S. Rajaraman, S. Parthasarathi, and S. Nestro, "Experimental investigation on mechanical properties of epoxy/graphene/fish scale and fermented spinach hybrid bio composite by hand lay-up technique," *Materials Today: Proceedings*, vol. 37, no. 2, pp. 1578–1583, 2021.

[22] D. J. Goodwin, S. Sepassi, and S. M. King, "Characterization of polymer adsorption onto drug nanoparticles using depletion measurements and small-angle neutron scattering," *Molecular Pharmacology*, vol. 10, no. 11, pp. 4146–4158, 2013.